The Dynamics of Protein Hydration Water: A Quantitative Comparison of Molecular Dynamics Simulations and Neutron-scattering Experiments

Mounir Tarek* and Douglas J. Tobias†

*National Institute of Standards and Technology, Center for Neutron Research, Gaithersburg, Maryland 20899-8562 and Department of Chemistry, University of Pennsylvania, Philadelphia, Pennsylvania 19104-6323 and †Department of Chemistry and Institute for Surface and Interface Science, University of California, Irvine, California 92697-2025 USA

ABSTRACT We present results from an extensive molecular dynamics simulation study of water hydrating the protein Ribonuclease A, at a series of temperatures in cluster, crystal, and powder environments. The dynamics of protein hydration water appear to be very similar in crystal and powder environments at moderate to high hydration levels. Thus, we contend that experiments performed on powder samples are appropriate for discussing hydration water dynamics in native protein environments. Our analysis reveals that simulations performed on cluster models consisting of proteins surrounded by a finite water shell with free boundaries are not appropriate for the study of the solvent dynamics. Detailed comparison to available x-ray diffraction and inelastic neutron-scattering data shows that current generation force fields are capable of accurately reproducing the structural and dynamical observables. On the time scale of tens of picoseconds, at room temperature and high hydration, significant water translational diffusion and rotational motion occur. At low hydration, the water molecules are translationally confined but display appreciable rotational motion. Below the protein dynamical transition temperature, both translational and rotational motions of the water molecules are essentially arrested. Taken together, these results suggest that water translational motion is necessary for the structural relaxation that permits anharmonic and diffusive motions in proteins. Furthermore, it appears that the exchange of protein–water hydrogen bonds by water rotational/librational motion is not sufficient to permit protein structural relaxation. Rather, the complete exchange of protein-bound water molecules by translational displacement seems to be required.

INTRODUCTION

Water plays a vital role in determining the structures and dynamics, and hence the function, of globular proteins. Water molecules in protein solutions may be broadly classified into three categories (Denisov and Halle, 1996; Bryant, 1996): strongly bound, internal water molecules that occupy internal cavities and deep clefts; water molecules that interact with the protein surface; and bulk water. Internal waters, which can be identified crystallographically and are conserved in homologous proteins (Rupley and Careri, 1991; Meyer, 1992; Williams et al., 1994), are extensively hydrogen bonded and comprise an integral part of the protein structure. They have residence times ranging from ~10 ns to ms, and their exchange with the bulk solvent requires local unfolding to occur (Denisov and Halle, 1995). Surface water molecules are much less well defined structurally than internal water molecules (in the sense that surface binding sites identified crystallographically are not highly conserved among different crystal forms of the same protein), and are much more mobile, with residence times on the order of tens of picoseconds (Halle, 1999b). In addition to being important for protein stability, and in the energetics and specificity of ligand binding, surface waters also have a profound influence on the dynamics of a protein molecule as a whole.

Globular proteins require a threshold level of hydration, $h \approx 0.4$ g H_2O per g dry protein, to function (Rupley and Careri, 1991). Although the details of the connection between protein hydration and function have not yet been worked out, it is clear that surface water is required for the activation of fast conformational fluctuations (Goldanskii and Krupyanskii, 1989; Ferrand et al., 1993; Fitter et al., 1997; Doster and Settles, 1999) that appear to be important in protein folding and function (Rasmussen et al., 1992; Ferrand et al., 1993; Barron et al., 1997). The observation of enzyme activity in partially hydrated powders (albeit lower activity than in solution) (Rupley and Careri, 1991), where the amount of water present is far less than sufficient to completely cover the protein surface, suggests a crucial role for the water molecules in the first hydration shell. Consequently, it is of interest to characterize the dynamical properties of this so-called protein hydration water in detail, and to investigate their potential connection to functionally relevant protein motions.

Numerous experimental and theoretical studies have demonstrated that the properties of protein hydration water are different from those of bulk water. X-ray and neutron diffraction experiments clearly indicate that the solvent structure in the vicinity of biomolecules differs from that of the bulk solvent (Teeter, 1991; Jiang and Brünger, 1994; Phillips and Pettitt, 1995; Burling et al., 1996; Rupley and Careri, 1991; Badger and Caspar, 1991; Wlodawer, 1982; Cheng and Schoenborn, 1990). Single particle dynamics of interfacial water has been studied extensively by nuclear magnetic relaxation techniques (Halle, 1999a,b). Analysis of ^{17}O and ^{2}H magnetic relaxation dispersion (MRD) ex-

Received for publication 27 March 2000 and in final form 30 August 2000.

Address reprint requests to Douglas J. Tobias, Department of Chemistry, University of California, Irvine, California 92697-2025. Tel.: 949-824-4295; Fax: 949-824-8571; E-mail: dtobias@uci.edu.

0006-3495/00/12/3244/14 $2.00

periments has demonstrated that the rotational motion of hydration water is slowed down by about a factor of five compared to bulk water (Denisov and Halle, 1995, 1996, 1998). Information about the translational motion of water, derived from the rate of intermolecular spin relaxation (Polnaszek and Bryant, 1984; Steinhoff et al., 1993) indicated a slower motion on the surface of proteins, in agreement with long residence times in the first hydration shell estimated from nuclear Overhauser enhancement (NOE) spectroscopy (Otting and Wüthrich, 1989; Otting et al., 1991; Otting, 1997).

Inelastic neutron scattering is a particularly useful approach to studying the dynamics of water at the surface of biomolecules (Randall et al., 1978; Middendorf, 1984, 1996; Bellissent-Funel, 2000). Incoherent neutron-scattering probes primarily the single particle motions of H atoms on length scales the order of Ångstroms and time scales ranging from picoseconds to nanoseconds. To take full advantage of neutron-scattering contrast through H/D substitution, biosynthetically deuterated hydrated proteins were studied by different authors (Randall et al., 1978; Middendorf, 1996; Bellissent-Funel et al., 1996). Most of the experiments on deuterated proteins have been reported on C-phycocyanin (CPC), a multimeric chromoprotein. In analogy with bulk supercooled water and water confined in microporous media such as vycor glass (Bellissent-Funel et al., 1993), incoherent neutron-scattering data for CPC hydration water (Bellissent-Funel et al., 1996) were interpreted on the basis of two classes of microscopic models. In the first, the translational and rotational water motions are assumed to be decoupled, the translational motion is described as diffusion in a confined space (e.g., a sphere) at a given site, along with jump diffusion between sites, and the rotational motion as rotational diffusion. This model leads to analytical expressions for the structure factors, which are then fit to the data, affording dynamical parameters such as the residence time at a given site, the jump length, and the translational and rotational diffusion constants. Bellissent-Funel et al. suggested that the water dynamics could also be described in terms of an α-relaxation model such as that applied to kinetic glass transitions in dense supercooled liquids, in analogy with their findings for water adsorbed in vycor glass (Zanotti et al., 1999). Settles and Doster (1996) reached similar conclusions in their study of hydrated myoglobin, in which they determined the intermediate scattering function and the mean squared displacement of hydration water by inverting incoherent neutron-scattering data. Their results clearly demonstrated the anomalous character of the diffusion of water at the protein surface.

More recently, molecular dynamics (MD) simulation studies of hydration water have been analyzed along these lines (Bizzarri et al., 1996; Bizzarri and Cannistraro, 1996, 1997; Rocchi et al., 1998), and have provided a detailed description of the spatial and temporal inhomogeneities that are at the roots of the anomalous behavior observed experimentally. Moreover, based on a MD simulation, Paciaroni et al. (1998) predicted the presence of a low-frequency vibrational anomaly, the so-called boson peak, typical of glassy materials, which was subsequently confirmed by neutron scattering (Paciaroni et al., 1999). Although, in recent MD simulation studies, qualitative agreement with results from neutron-scattering experiments has been demonstrated, the lack of quantitative agreement, exposed below in this paper, casts some doubt on their conclusions. The disagreement has been blamed primarily on the inadequacy of current-generation force fields to accurately reproduce the water dynamical properties.

In this paper, we report an extensive molecular dynamics simulation study of water dynamics near a protein surface. We focus our attention primarily on making a detailed comparison with incoherent inelastic neutron-scattering experiments on hydrated protein powders, and show, for the first time, that it is possible to obtain quantitative agreement with most available data. We address outstanding issues concerning the interpretation of neutron-scattering experiments, such as the relevance of powder results to native environments, and the validity of the analysis of neutron data in terms of microscopic diffusive models. From the simulation standpoint, we address the subtleties of comparing MD results to neutron experiments, identify problems related to an inappropriate representation of the protein environment, and examine the dependence of the results on the choice of the water model. To these ends, we present results from simulations of hydrated Ribonuclease A at several temperatures in cluster, crystal, and powder environments, and compare them to results from inelastic neutron-scattering experiments and previous simulations. Finally, we discuss the connection between water and protein dynamics in light of the obtained results.

COMPUTATIONAL DETAILS

Bulk water

MD simulations of bulk water were performed with the TIP3P (Jorgensen et al., 1983) and SPC/E (Berendsen et al., 1987) models at 300 K and zero pressure. Both simulations were initiated from a previously equilibrated system containing 401 TIP3P water molecules in a 24-Å cubic box. The simulations were run for 400 ps, and the last 100 ps were used for analysis. The average densities from the TIP3P and SPC/E simulations were 1.012 g/cm^3 and 0.999 g/cm^3, respectively, which should be compared to the experimental value of 0.997 g/cm^3 at 298 K (Weast, 1971).

Protein/water cluster

MD simulations of a hydrated RNase cluster were carried 150 K and 300 K. The TIP3P water model (Jorgensen et al., 1983) was used, and the water hydrogen masses were set to

correspond to D_2O. The initial protein configuration was the crystal coordinates in the file 7RSA (Wlodawer et al., 1988) from the Protein Data Bank. After energy minimization, the protein was placed in a box of water large enough to accommodate the protein plus approximately three shells of water, and the resulting system was subjected to 10 ps MD at constant volume. All but the 399 water molecules closest to the protein were removed, giving a hydration level, $h = 0.58$ g D_2O per g protein. The resulting protein/water cluster was simulated at constant volume and temperature in a $70 \times 70 \times 60$ Å box with periodic boundary conditions so that the Ewald sum could be used to calculate the electrostatic energies and forces without truncation. The cluster simulations were run for 3000 ps.

Crystals

The crystal simulations contained two RNase and 817 water molecules, giving a hydration level, $h = 0.59$ g D_2O per g protein. Protein crystal structures generally contain some water molecules, but these constitute a small fraction of the total number of waters in the crystal. Thus, we prepared our system in a series of stages that involved addition of water molecules, followed by annealing with constant volume MD. First, the monoclinic unit cell containing two protein molecules was generated from the asymmetric unit (one molecule), by using the symmetry operations of the $P2_1$ space group. The empty space in the cell was filled with water molecules, and the positions of the waters were relaxed by energy minimization and MD with periodic boundary conditions until the pressure stabilized in the field of the protein molecules, whose positions were held fixed. Interactions of the water molecules with each other and the proteins opened new vacancies for additional water molecules. The procedure of adding water molecules was repeated until there was no more empty space in the unit cell (six addition/annealing cycles).

The crystal was subsequently simulated with TIP3P D_2O at constant pressure and temperature for 1700 ps at 300 K, and 700 ps at 250, 200, 150, and 100 K. The masses on the water deuterium atoms were set to the mass of a hydrogen atom and the simulations were continued for an additional 200 ps at each temperature. Then the water force field parameters were set to those of the SPC/E model, and the simulations were run for another 200–400 ps at each temperature.

Powders

Three model RNase powder systems, two of which we shall refer to as ordered powders (OP), and the other as a random powder (RP), were simulated at 300 K. Both the OP and RP powders contain eight protein molecules replicated by periodic boundary conditions (so that they are actually polycrystalline), but they have completely different protein configurations and protein–protein interactions, and significantly different water pockets and channels. A comparison of the two systems is therefore useful for assessing the importance of the details of the molecular packing in powder environments. To construct the OP systems, we began with 4-unit cells (a $2a \times 2b \times c$ lattice) of the monoclinic crystal with the water molecules removed, and ran constant volume MD at 500 K to produce non-native, disordered configurations on the surfaces of the protein molecules. This was followed by a constant pressure run at 300 K, during which the system contracted, enabling the protein molecules to interact with their neighbors and periodic images. The OP system was hydrated to $h = 0.05$ g D_2O per g protein and 0.42 g D_2O per g protein by adding 280 and 2188 water molecules, respectively, to empty spaces in configurations selected from the constant pressure run. The RP system was prepared by exactly the same procedure as the high-hydration OP system, but starting from a completely different initial arrangement obtained by randomly rotating and then repacking the protein molecules before heating.

The low-hydration OP, high-hydration OP, and RP systems were simulated with TIP3P D_2O at constant pressure and temperature for 750, 1000, and 300 ps, respectively, at 300 K. The high hydration OP simulation was run for an additional 200 ps with the deuterium atoms changed to hydrogen. The water potential parameters were subsequently changed to those of the SPC/E model, and the simulation was continued for another 200 ps.

Details of the simulations

A summary of the 15 protein/water systems simulated is given in Table 1. The CHARMM 22 force field (MacKerell et al., 1998) was used for the protein. Three-dimensional periodic boundary conditions were applied and the Ewald sum was used to calculate the electrostatic energies, forces, and virial in all of the simulations. The Lennard–Jones interactions and the real-space part of the Ewald sum were smoothly truncated at 10 Å, and long-range corrections to account for the neglected interactions were included in the energies and pressures (Allen and Tildesley, 1989). The reciprocal space part of the Ewald sum was calculated using the smooth particle mesh method (Essmann et al., 1995). The Nosé–Hoover chain method (Martyna et al., 1992) was used to the control the temperature in all of the simulations, with separate thermostat chains for the water and protein molecules. The constant pressure simulations were carried out in a fully flexible simulation box by using the algorithm of Martyna et al. (1994). A multiple time step algorithm (Martyna et al., 1996) was used to integrate the equations of motion with a 4 fs time step. The lengths of bonds involving H/D atoms were held fixed by using the SHAKE/RATTLE algorithm (Ryckaert et al., 1977; Andersen, 1983).

TABLE 1 Summary of the protein/water systems simulated

Simulation	Environment*	T (K)	Water Model†	Number of RNase Molecules	Number of Water Molecules	Hydration Level‡	Run Length (ps)§
A	cluster	300	TIP3P (D)	1	399	0.58	3000
B	cluster	150	TIP3 (D)	1	399	0.58	3000 (A)
C	crystal	300	TIP3P (D)	2	817	0.59	1700
D	crystal	300	TIP3P (H)	2	817	0.53	200 (C)
E	crystal	300	SPC/E (H)	2	817	0.53	400 (D)
F	crystal	250	TIP3P (D)	2	817	0.59	700 (C)
G	crystal	150	TIP3P (D)	2	817	0.59	700 (C)
H	crystal	150	TIP3P (H)	2	817	0.53	200 (G)
I	crystal	150	SPC/E (H)	2	817	0.53	400 (H)
J	crystal	100	TIP3P (D)	2	817	0.59	700 (C)
K	OP	300	TIP3P (D)	8	2188	0.42	750
L	OP	300	TIP3P (H)	8	2188	0.38	200 (K)
M	OP	300	SPC/E (H)	8	2188	0.38	200 (L)
N	OP	300	TIP3P (D)	8	280	0.05	1000
O	RP	300	TIP3P (D)	8	2188	0.42	300

*OP and RP refer to the ordered and random powders, respectively. See text for details.
†Letter in parentheses denotes whether hydrogen (H) or deuterium (D) masses were used for the water hydrogen atoms.
‡Hydration level is defined as g H_2O or g D_2O per g protein.
§Letter in parentheses refers to the previous simulation from which the run was initiated.

Analysis methodology

Numerical solution of the equations of motion in MD simulations produces phase–space trajectories that consist of the positions and momenta (velocities) of all the atoms in the system as a function of time. A variety of ensemble-averaged quantities that correspond to experimental observables may be computed from these trajectories. In this paper, we focus on quantities related to incoherent neutron-scattering measurements that probe motions of hydrogen atoms on picosecond time scales.

Most neutron spectroscopy experiments essentially measure the total dynamic structure factor, $S_{\mathrm{tot}}^{\mathrm{meas}}(\mathbf{Q}, \omega)$, in which $\mathbf{Q}$ and $\hbar\omega$ are the momentum and energy transfers, respectively. The measured structure factor is the sum of coherent and incoherent contributions. However, because the incoherent scattering length of hydrogen is an order of magnitude larger than the scattering lengths of all the other atoms in proteins and water molecules, we assume that the coherent contribution is negligible, so that $S_{\mathrm{tot}}^{\mathrm{meas}}(\mathbf{Q}, \omega) = S_{\mathrm{inc}}^{\mathrm{meas}}(\mathbf{Q}, \omega)$. In practice, the spread in energies of the neutrons incident on the sample results in a finite energy resolution, and the measured spectrum is a convolution of the true spectrum, $S_{\mathrm{inc}}(\mathbf{Q}, \omega)$, and the instrumental resolution function, $R(\omega)$:

$$S_{\mathrm{inc}}^{\mathrm{meas}}(\mathbf{Q}, \omega) = S_{\mathrm{inc}}(\mathbf{Q}, \omega) \otimes R(\omega), \tag{1}$$

where $\otimes$ denotes a convolution product. The width of the resolution function determines the time scale of the dynamics probed by the instrument in a nontrivial way, with narrower widths (higher resolution) corresponding to longer observation times.

From the theory of neutron scattering (Beé, 1988), $S_{\mathrm{inc}}(\mathbf{Q}, \omega)$ may be written as the Fourier transform of a time correlation function, the "intermediate scattering function," $I_{\mathrm{inc}}(\mathbf{Q}, t)$:

$$S_{\mathrm{inc}}(\mathbf{Q}, \omega) = \frac{1}{2\pi}\int_{-\infty}^{\infty} I_{\mathrm{inc}}(\mathbf{Q}, t)e^{-i\omega t}\,dt; \tag{2}$$

$$I_{\mathrm{inc}}(\mathbf{Q}, t) = \langle \exp^{i\mathbf{Q}\cdot\mathbf{r}_i(t)} \exp^{-i\mathbf{Q}\cdot\mathbf{r}_i(0)} \rangle. \tag{3}$$

Here, $\mathbf{r}_j$ is the position operator of atom j, or, if the correlation function is calculated classically, as in an MD simulation, $\mathbf{r}_j$ is a position vector, and the angle brackets denote an average over time origins and scatterers (i.e., H atoms). Note that, in Eq. 3, we have left out a factor equal to the square of the scattering length. This is convenient in the case of a single dominant scatterer because it gives $I(\mathbf{Q}, 0) = 1$ and $S_{\mathrm{inc}}(\mathbf{Q}, \omega)$ normalized to unity. The intermediate scattering function, $I_{\mathrm{inc}}(\mathbf{Q}, t)$, is readily computed from an MD trajectory by using Eq. 3, and the result may be numerically Fourier transformed to afford $S_{\mathrm{inc}}(\mathbf{Q}, \omega)$.

To quantitatively compare spectra computed from MD simulations to neutron-scattering data taken on a given spectrometer, we have taken the instrumental resolution into account. Instrumental resolution functions are generally represented by a Gaussian or other peaked function, centered at $\omega = 0$, with width $\Delta\omega$ (or $\Delta E = \hbar\Delta\omega$). Noting that a convolution in energy space is equivalent to a product in the time domain, we compute resolution-broadened spectra, $S_{\mathrm{inc}}^{\mathrm{meas}}(\mathbf{Q}, \omega)$, by Fourier-transforming the product, $I_{\mathrm{inc}}(\mathbf{Q}, t)R(t)$, where $R(t)$ is the Fourier transform of $R(\omega)$.

The $I(Q, t)$ (and their corresponding spectra) reported in this paper are "powder averages" of $I_{inc}(\mathbf{Q}, t)$ computed at eight randomly chosen scattering vectors with $|\mathbf{Q}| = Q$.

We shall examine the details of the shapes of the neutron-scattering spectra, which are sensitive to the nature of diffusive motions. To this end, it is useful to consider the imaginary part of the dynamical susceptibility, $\chi''(Q, \omega)$, which, in the classical limit may be written,

$$\chi''(Q, \omega) = \frac{\beta\omega}{2} S(Q, \omega), \tag{4}$$

where $\beta = 1/k_B T$ (Boon and Yip, 1991). We will compare susceptibilities for water protons computed from our MD trajectories to those measured in myoglobin powders by Settles and Doster (1996).

To characterize diffusive motion in the time domain, we will use the intermediate scattering functions $I(Q, t)$, and the atomic mean-squared displacements (MSD),

$$\mathrm{MSD}(t) = \langle |\mathbf{r}_j(t) - \mathbf{r}_j(0)|^2 \rangle. \tag{5}$$

To discuss water rotational motion, we will refer to the second rank rotational correlation functions, $C(t)$:

$$C(t) = \langle P_2[\mathbf{u}(t) \cdot \mathbf{u}(0)] \rangle, \tag{6}$$

where $\mathbf{u}$ is a unit vector in the direction of a water dipole, and $P_2(x) = \frac{1}{2}(3x^2 - 1)$.

The majority of incoherent neutron scattering in protein/water systems arises from proton motions. The water contribution contains information on both translational and rotational motion, which are usually assumed to be decoupled in the fitting and interpretation of the experimental data. Following Chen et al. (1997) in their MD simulation study of bulk supercooled water, we will address the validity of this assumption for protein hydration water by examining the coupling contribution to the intermediate scattering function, $I(Q, t) - I_{trans}(Q, t)I_{rot}(Q, t)$, where $I_{trans}(Q, t)$ and $I_{rot}(Q, t)$ are the translational and rotational contributions to the intermediate scattering functions, respectively:

$$I_{trans}(Q, t) = \langle \exp^{i\mathbf{Q}\cdot\mathbf{R}_j(t)} \exp^{-\mathbf{Q}\cdot\mathbf{R}_j(0)} \rangle, \tag{7}$$

$$I_{rot}(Q, t) = \langle \exp^{i\mathbf{Q}\cdot\mathbf{b}_j(t)} \exp^{-\mathbf{Q}\cdot\mathbf{b}_j(0)} \rangle, \tag{8}$$

where $\mathbf{R}_j$ is the position of the center-of-mass of the jth water molecule, and $\mathbf{b}_j$ is the position of the jth hydrogen atom from the center-of-mass (i.e., $\mathbf{b} = \mathbf{r} - \mathbf{R}$).

To discuss localized (as opposed to diffusive) motions, it is useful to isolate the phonon contribution to the experimental structure factor into the vibrational density of states (DOS), $g(\omega)$. Because the short-time behavior of a molecule in a liquid may be described as oscillatory motion in the cage formed by its neighbors, the water density of states may be computed from a simulation trajectory as the Fourier transform of the proton velocity autocorrelation function, $C_{vv}(t)$, by analogy to a solid of independent harmonic oscillators, i.e.,

$$g(\omega) = \frac{1}{2\pi} \int_{-\infty}^{\infty} C_{vv}(t) e^{-i\omega t}\, dt, \tag{9}$$

$$C_{vv}(t) = \langle \mathbf{v}_j(0) \cdot \mathbf{v}_j(t) \rangle. \tag{10}$$

We will compare our computed water proton densities of states to those measured by neutron scattering for C-phycocyanin powders by Bellissent-Funel et al. (1996).

RESULTS AND DISCUSSION

Protein structure and lattice parameters

Before presenting results concerning the water dynamics, we briefly compare the protein structures and lattice parameters from the simulations to those determined by x-ray diffraction (Wlodawer et al., 1988; Tilton et al., 1992) to assess the quality of the force fields and simulation methodology. In Table 2, we compare the experimental unit cell parameters at several temperatures with those computed from the last 100 ps of constant pressure MD simulations in which all the parameters were allowed to vary. It is clear that, overall, the simulation results are in very good agreement with the experimental values. In all cases, the monoclinic symmetry is well maintained, and the experimentally observed shrinkage of the cell lengths with decreasing temperature is well tracked by the simulations. The maximum deviations between the experimental and simulated values of the cell lengths and angles is ~4% and 5%, respectively, at 300 K, and the agreement between the simulated and experimental results improves at lower temperatures. A comparison of the simulations with the TIP3P and SPC/E water models at 300 K shows that the differences between the two models have negligible effects on the overall structure of the crystal.

To assess the ability of the simulations to maintain the correct internal structure of the protein molecules, we have computed the root mean squared deviations (RMSDs) of the C^α positions in the simulations versus the 1.26-Å resolution crystal structure of Wlodawer et al. (1988). The C^α atoms define the backbone of the protein molecule. In Table 3, we compare average RMSDs computed over the last 100 ps of the cluster, crystal, and high-hydration powder simulations. In every case, the RMSDs had converged before the averaging period in the sense that they exhibited small fluctuations in time about their averages, which were not drifting. The cluster and crystal RMSDs of 1.3–1.4 Å are typical deviations for current-generation, all-atom protein force fields, and indicate that the overall protein structure is reasonably well maintained during the simulations. Comparison of the crystal results obtained with the TIP3P and SPC/E water models shows that the differences between the

TABLE 2 Comparison of X-ray diffraction and constant pressure MD values for the unit cell parameters of the monoclinic Ribonuclease A crystal*

Source†	T (K)	a (Å)	b (Å)	c (Å)	α (°)	β (°)	γ (°)
X-ray‡	300	30.18	38.40	53.32	90.0	105.8	90.0
X-ray§	300	30.27	38.43	53.79	90.0	107.9	90.0
MD (TIP3P)	300	31.43_{24}	38.02_{26}	51.56_{45}	90.0_{6}	112.8_{6}	89.3_{8}
MD (SPC/E)	300	31.45_{13}	37.85_{19}	52.04_{28}	90.0_{5}	112.2_{4}	89.8_{4}
X-ray§	260	30.16	38.18	53.14	90.0	106.4	90.0
MD (TIP3P)	250	29.99_{15}	37.60_{22}	52.57_{34}	92.1_{4}	108.3_{5}	90.0_{5}
X-ray§	160	29.51	38.08	52.93	90.0	106.3	90.0
MD (TIP3P)	150	29.48_{06}	37.88_{08}	51.87_{10}	91.2_{2}	108.4_{2}	90.0_{2}
X-ray§	98	29.48	38.08	52.97	90.0	106.1	90.0
MD (TIP3P)	100	29.38_{05}	37.80_{06}	51.75_{08}	91.3_{1}	108.2_{1}	89.9_{1}

*MD values are averages over the last 100 ps of the respective simulations. Subscripted numbers are standard deviations in the last significant digits.
†The water model used in the MD simulations is given in parentheses.
‡(Wlodawer et al., 1988).
§(Tilton Jr. et al., 1992).

water models have little influence on the overall protein structure. The range of RMSDs for the eight protein molecules in the powders, 2.05–2.72 Å in the OP, and 2.13–3.42 Å in the RP, are significantly greater than the values in the crystal. This demonstrates that we have succeeded in generating protein structures with significant deviations from the native structure in our powder models. Comparing the RMSDs in the two powders, it appears that the deviations in the RP are systematically larger than those in the OP, by about 0.2 Å, on average.

Environmental dependence of the water dynamics

Before proceeding to an in-depth analysis of our simulation results, including a detailed comparison with experimental results, we briefly compare results concerning the overall water dynamics in cluster, crystal, and powder environments. This comparison is useful for two reasons. First, it provides a basis for assessing the relevance of neutron-scattering measurements that are typically performed on partially hydrated powder samples to fully hydrated proteins in the native-like crystal environment. Second, it exposes significant dynamical artifacts due to the absence of the surroundings in simulations of the cluster models that are commonly used to study protein and water dynamics. Because we are exclusively concerned with the environmental dependence, we shall restrict our attention in this section to the most extensive series of simulations performed with the same water model, namely, those with the TIP3P model for D_2O. A detailed comparison with experimental results for H_2O, including an investigation of the results on the water potential, is reported in the following section.

In Figs. 1 and 2, we compare the mean-squared displacements, and the intermediate scattering functions, $I(Q = 1.4\ \text{Å}^{-1}, t)$, computed for the deuterium atoms in the simulations of the cluster (simulation A in Table 1), crystal (B), ordered powder (J), and random powder (N) systems at 300 K. We make two observations concerning these data (results for other values of the scattering vector are qualitatively similar (Tarek and Tobias, 1999)): (1) the MSDs and $I(Q, t)$ are very similar on the time scale of tens of picoseconds in the crystal and the two structurally distinct powder models, and this implies that, on this time scale, the overall water motion is insensitive to the details of the protein packing at moderate to full hydration ($h > 0.4$); (2) $I(Q, t)$ decays much too rapidly (i.e., the water molecules move much too freely) in the cluster compared to the crystal and powders due to the absence of the surroundings of a realistic, bulk environment.

In Fig. 3, we show velocity autocorrelation functions (VACFs) and the corresponding DOS computed for the TIP3P deuterium atoms from the simulations of the cluster, crystal, and high hydration OP at 300 K. All of the VACFs

TABLE 3 Root-mean squared deviations (in Å) of the Ribonuclease A C^{α} positions from MD simulations (averaged over the last 100 ps) versus the experimental crystal structure (Wlodawer et al., 1988) at 300 K*

Molecular Number	Cluster (TIP3P)	Crystal (TIP3P)	Crystal (SPC/E)	High Hydration OP (TIP3P)	High Hydration RP (TIP3P)
Individual values by molecule	1.31	1.34, 1.40	1.39, 1.44	2.05, 2.08, 2.33, 2.34, 2.39, 2.63, 2.71, 2.72	2.13, 2.46, 2.46, 2.65, 2.88, 3.15, 3.37, 3.42
Average	1.31	1.37	1.42	2.40	2.55

*The water model used in the MD simulations is given in parentheses.

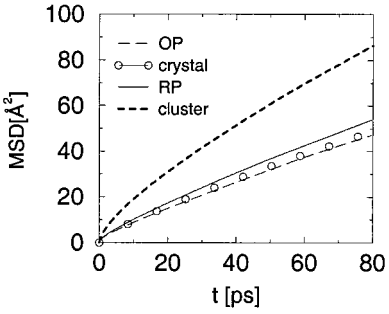

FIGURE 1 Mean-squared displacements computed for water D atoms from MD simulations of RNase A hydrated with the TIP3P model of D_2O in the "ordered powder" (OP), crystal, "random powder" (RP), and cluster environments at 300 K.

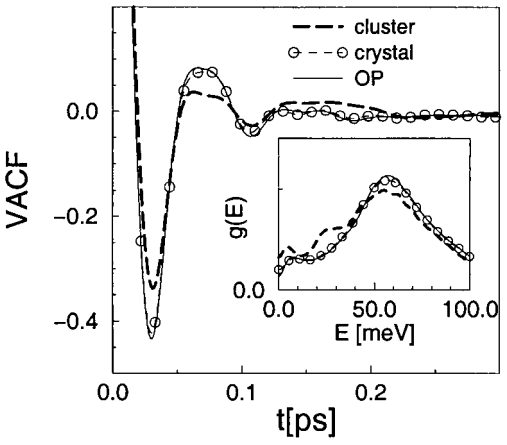

FIGURE 3 Velocity autocorrelation functions computed for water H atoms from MD simulations of RNase A hydrated with the TIP3P model of H_2O in the "ordered powder" (OP), crystal, and cluster environments at 300 K. The inset shows the corresponding frequency distributions (density of states), $g(E = \hbar\omega)$, obtained by Fourier transforming the VACFs.

display damped oscillations that are typical of the protons in liquid water. A detailed comparison with the bulk will be presented in the next section. From Fig. 3 it is evident that the short-time (<0.5 ps) dynamics of the water protons, as reflected in the VACFs, are virtually identical in the crystal and powder. In contrast, in the cluster, the VACF is more strongly damped compared to the condensed environments. The DOS of the water protons computed from the crystal and powder VACFs are essentially the same, both containing a small peak assigned to translational motion at ≈6 meV, and a more pronounced, broad librational peak centered at ≈55 meV. The DOS for the water protons in the cluster differs from those in the crystal and powder in two significant respects. First, both the translational and librational peaks are shifted to lower energies. In addition, the cluster result contains a pronounced peak at ≈20 meV that is not observed in the crystal and powder results.

An additional perspective on the differences in the low frequency dynamics of protein hydration water between the cluster and crystal environments is provided by the dynamical susceptibility spectra plotted in Fig. 4. In qualitative agreement with spectra for protein hydration water measured by neutron scattering at low temperature (180 K) (Settles and Doster, 1996), the spectra from the simulations at 150 K display three prominent features in addition to the resolution-broadened elastic peak below 0.2 meV: a translational band (TA_1) around 4 meV, the librational peak around 40 meV, and a deep minimum between the elastic peak and the translational band where the α-resonance, corresponding to diffusive structural relaxation, is observed in bulk water spectra. Comparing the cluster and crystal spectra at 150 K (Fig. 4), we see that the TA_1 band of the cluster spectrum is broader, shifted to lower frequencies, and contains more intensity than that of the crystal spectrum, and the minimum is shallower, indicating an enhancement of local diffusive motions in the cluster compared to the crystal. In addition, the cluster spectrum contains a small, spurious band at approximately 20 meV that is not seen in the crystal spectrum at 150 K. An extra peak near 20

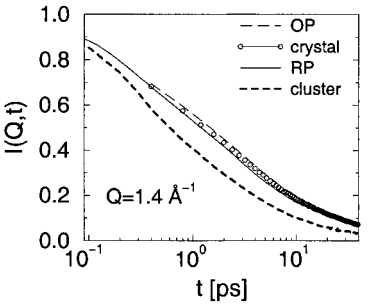

FIGURE 2 Incoherent (self) intermediate scattering functions computed at $Q = 1.4$ Å^{-1} for water D atoms from MD simulations of RNase A hydrated with the TIP3P model of D_2O in the "ordered powder" (OP), crystal, "random powder" (RP), and cluster environments at 300 K.

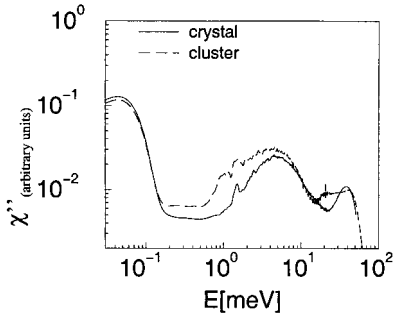

FIGURE 4 Imaginary part of the dynamical susceptibility spectrum computed at $Q = 2$ Å^{-1} for water D atoms from MD simulations of RNase A hydrated with the TIP3P model of D_2O in the crystal and cluster environments at 150 K.

meV has also been observed in susceptibility spectra computed from MD simulations of a plastocyanin/water cluster at 100 and 200 K (Paciaroni et al., 1998). The lack of quantitative agreement between the simulation results in Fig. 4 and the neutron-scattering data of Settles and Doster (1996) will be addressed in the following section.

Taken together, the results presented in this section suggest that the dynamics of protein hydration water is very similar in crystal and powder environments at moderate to high hydration levels. Thus, we contend that experiments performed on powder samples are appropriate for discussing hydration water dynamics in native protein environments (and vice versa). Therefore, in what follows, we will concentrate primarily on results from our crystal simulations, and assume that our conclusions are applicable to powder samples at the same hydration level. Moreover, the results in this section demonstrate definitively that simulations of a cluster give significantly different results compared to simulations of crystals/powders. We now proceed to an assessment of the quantitative validity of the water dynamics in our crystal simulations by comparing them to data from neutron-scattering experiments.

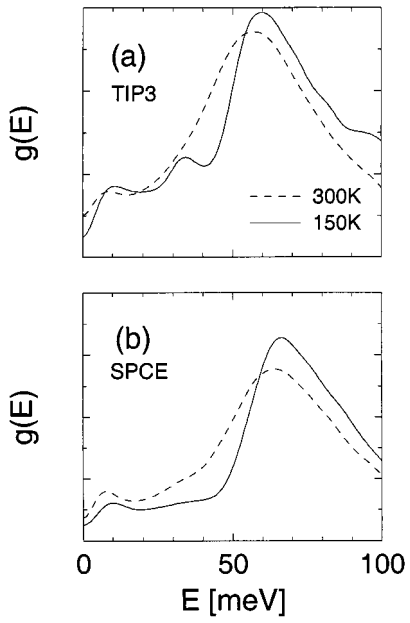

FIGURE 5 Vibrational density of states, $g(E = \hbar\omega)$, computed for the water H atoms from the MD simulations of RNase A crystals at 300 K (*dashed lines*) and 150 K (*solid lines*). (a), with TIP3P model of H_2O, and (b) with SPCE model of H_2O.

Comparison with neutron-scattering experiments and water model dependence

In the previous section, we used results from a large set of simulations performed with the TIP3P water model for D_2O to discuss qualitative differences in water dynamics in different protein environments. In this section, we compare our results to incoherent neutron-scattering experiments that probe the motions of H atoms, and hence we focus primarily on the smaller set of simulations carried out with H_2O. In the analysis of our initial results for TIP3P H_2O, we found poor agreement with the neutron data. We therefore performed additional simulations with SPC/E H_2O to investigate the dependence of the results on the water model. As we shall see in this section, the SPC/E model gives much better agreement with the neutron data. We compare our simulation results for water in the ribonuclease A crystal with neutron data on CPC, myoglobin, and plastocyanin powders. For the most part, we expect the average single-particle dynamics of hydration water probed by neutrons to be similar for different soluble proteins, and hence we seek close agreement between our results and data from various experiments.

In Fig. 5, we show the proton densities of states (computed according to Eq. 8) for the two water models in the RNase crystal at 150 and 300 K. These results may be compared with neutron data on a CPC powder at 150 and 333 K (Bellissent-Funel et al., 1996). Both sets of simulation results display translational and rotational peaks in the vicinity of 7 and 65 meV, respectively, consistent with the experimental results, and both reproduce the experimentally observed red shift of the librational peak, and the "filling in" of the DOS between the two peaks, with increasing temperature. The slight red shift of the translational peak predicted by the simulations is not evident in the neutron spectra. The librational peaks in the SPC/E spectra occur a few meV higher in energy than in the TIP3 spectra, and are in better agreement with the neutron data. Moreover, there is a spurious peak around 35 meV in the TIP3P DOS at 150 K. Thus, the SPC/E model appears to provide a better representation for the short-time (<0.5 ps), localized motions of protein hydration water.

To illustrate the water model dependence of the diffusive motions over a range of length scales, in Fig. 6 we have plotted the intermediate scattering functions computed for the water protons in the RNase crystal at 300 K. The correlation functions for both water models show a two-step decay, the first involving fast single-particle dynamics in the cage formed by the neighboring particles, and the second to diffusive translational motion beyond the confines of the cage. The time scale of the initial decay displays a strong model dependence: for the TIP3P model it is complete in 0.1 ps, whereas for the SPC/E model it is an order of magnitude longer. The latter is in good agreement with experimental results obtained by deconvoluting and inverting structure factors for myoglobin hydration water at 320 K (Settles and Doster, 1996). The secondary decay at a given value of Q for the SPC/E model is significantly slower, and more consistent with the myoglobin data, than for TIP3P. However, the SPC/E correlation functions still decay too fast compared to those measured in myoglobin powders.

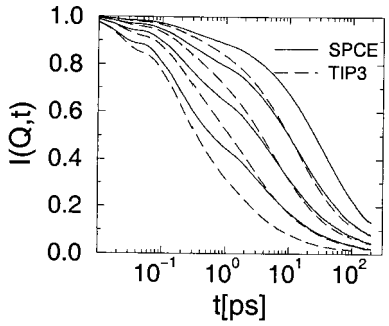

FIGURE 6 Incoherent (self) water H intermediate scattering functions computed (from top to bottom) at $Q^2 = 0.5$, 1.0, 2.0 and 4.0 Å^{-1}; from the MD simulations of RNase A crystals at 300 K, hydrated with the SPCE model (*solid lines*) and hydrated with the TIP3P model (*dashed lines*) of H_2O.

This may reflect the higher hydration level in the simulation (0.52 versus 0.35), or inadequacies of the force field or the use of the crystal as a model for the powders used in the experiments, or uncertainty in the inversion of the experimental data.

The secondary decay of the density correlation functions for protein hydration water is nonexponential. In fact, the decay is described well by a stretched exponential, which suggests spatial or temporal inhomogeneities in the single particle diffusive motion (Settles and Doster, 1996; Rocchi et al., 1998). In Fig. 7, we show fits of $I(Q, t)$ for the SPC/E protons from the 300 K RNase crystal simulation to a stretched exponential (Kohlrausch–Williams–Watts) form,

$$I_K(Q, t) = A(Q)\exp\left[-\left(\frac{t}{\tau}\right)^{\beta}\right]. \qquad (11)$$

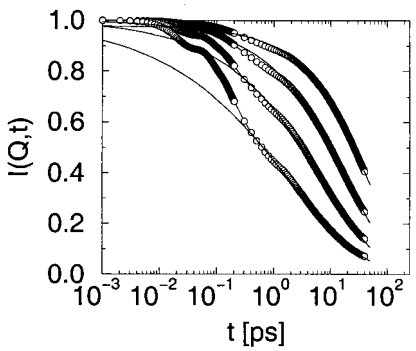

FIGURE 7 Incoherent (self) water H intermediate scattering functions computed (from top to bottom) at $Q^2 = 0.5$, 1.0, 2.0 and 4.0 Å^{-1}; from the MD simulations of the RNase A crystal at 300 K hydrated with the SPCE model (*circles*). The solid curves are fits to the stretched exponential function (Eq. 11)) between 2 ps and 40 ps.

The Q-dependence of the parameters τ and β, and the average relaxation time,

$$\langle\tau\rangle = \int_{-\infty}^{\infty} I_K(Q, t)/A(Q)\, dt = \frac{\tau}{\beta}\Gamma\left(\frac{1}{\beta}\right), \qquad (12)$$

are shown in Fig. 8. The data in Fig. 8 may be compared with the corresponding results from the neutron-scattering measurements on myoglobin powder (Settles and Doster, 1996). The neutron data were inverted by considering two limiting cases when subtracting the protein contribution to the scattering. In Case 1, the protein exchangeable protons were assumed to be dynamically equivalent to water protons, whereas in Case 2, they were considered to behave as nonexchangeable protons, and hence their contribution was removed by subtraction. The correlation functions obtained the Case 1 decay significantly slower (have smaller β and larger τ and $\langle\tau\rangle$) than for Case 2. The simulation results shown in Fig. 8 are in much better agreement with Case 2. The values of β from the simulation are slightly higher (by about 0.04) and the values of τ are about a factor of two too large compared to Case 2 over the range $Q = 1$–2 Å^{-1}.

Microscopic models used to interpret neutron-scattering data in terms of rotational and translational motion assume that these motions are decoupled, so that the overall intermediate scattering function is a product of rotational and translational contributions. We have used our simulations to investigate the validity of this assumption for the water protons in simulations of the RNase crystal. In Fig. 9, we show the total intermediate scattering function, its translational and rotational contributions, and the coupling contribution (the difference between the total and the product of

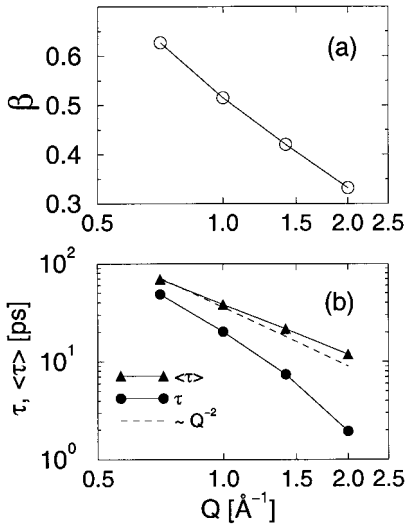

FIGURE 8 Q dependence of the parameters from the stretched exponential fits in Fig. 7: (a) stretching exponent, β; (b) time scale parameter, τ, and average correlation time, $\langle\tau\rangle$, defined by Eq. 12).

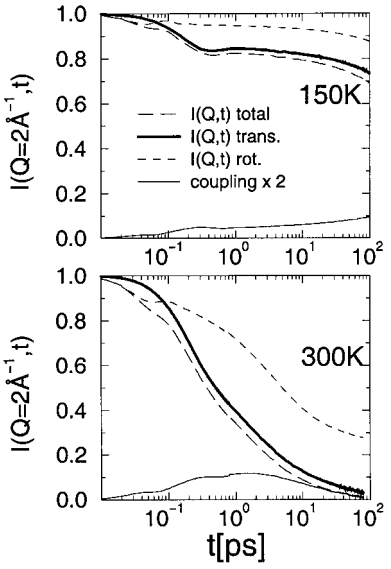

FIGURE 9 Translational (*bold solid lines*), rotational (*short dashed lines*), and coupling (*thin solid lines*) contributions to the total (*long dashed lines*) incoherent intermediate scattering functions computed at $Q = 2$ Å^{-1} for the D atoms of TIP3P D_2O in the RNase A crystals at 150 K and 300 K. The translational/rotational coupling has been scaled by a factor 2 for ease of viewing.

rotational and translational contributions) at 150 and 300 K for $Q = 2$ Å^{-1}. It is evident that, at this value of the momentum transfer, the coupling is appreciable, reaching a maximum of ~5% at ~1 ps at 300 K and at least 5% at much longer times (>100 ps) at 150 K. However, at a given temperature, the coupling rapidly diminishes with decreasing Q (data not shown). The time, temperature, and Q (length scale) dependence of the rotational-translational coupling observed in our simulations of protein hydration water are strikingly similar to those observed in MD simulations of bulk supercooled water (Chen et al., 1997). Thus, our simulations provide further support for the analogy between the dynamics of water molecules next to proteins and in the bulk supercooled state, and suggest that the conclusions of Chen et al. (1997) concerning the validity of microscopic models for the analysis of neutron data are also applicable to protein hydration water.

Dynamical susceptibility spectra provide information on diffusive motions over a broad frequency range. In Fig. 10, we have plotted the spectra computed for water protons from simulations of bulk water, and water in the RNase crystal at 150 and 300 K, using the SPC/E water model. The origin of the features in the spectra has been discussed in the previous section. The results in Fig. 10 may be compared with corresponding neutron-scattering data on myoglobin powders at a similar hydration level (Settles and Doster, 1996). The agreement between the results in Fig. 10 and the experimental data reported by Settles and Doster is excellent. The presence, locations, and temperature dependence

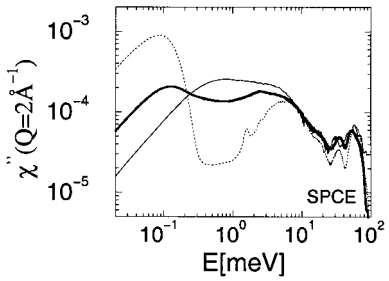

FIGURE 10 Water dynamical susceptibility spectra computed at $Q = 2$ Å^{-1} from the MD simulation of SPCE H_2O water in the bulk phase at 300 K (*thin solid line*), in the RNase A crystal at 300 K (*bold solid line*), and in the RNase A crystal at 150 K (*dotted line*).

of all the features (peaks and valleys) in the bulk and hydration water spectra are remarkably well reproduced by the simulations. Thus, we may conclude that, with the SPC/E water model and a reasonable representation of the environment in the samples studied experimentally, simulations are capable of accurately modeling the perturbation of water dynamics next to a protein surface.

The susceptibility representation reveals features that are not evident in the spectrum, $S(Q, \omega)$. However, there is one particularly interesting feature in the spectrum at low temperature that is obscured by the prominent TA_1 peak (at 7 meV) in the susceptibility. This is the so-called boson peak, a broad, low-energy inelastic feature observed at ≈3 meV in the low-frequency Raman and neutron-scattering spectra of many glassy systems, including globular proteins (Angell, 1995; Frick and Richter, 1995; Leyser et al., 1999). In Fig. 11, we have plotted the incoherent structure factor, $S(Q, E)$, for the water protons computed from a simulation of the RNase crystal at 150 K with the SPC/E water model. The boson peak is evident in the crystal spectrum as a broad excess of intensity, centered near 3 meV, over the harmonic background. Such a peak has been observed in the inelastic spectra of several proteins in D_2O, but was only recently predicted for hydration water in an MD simulation study

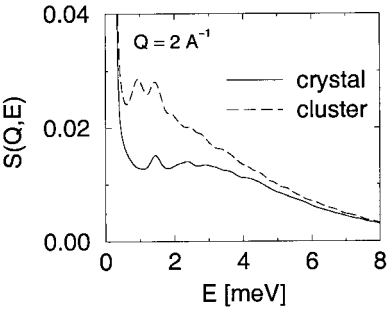

FIGURE 11 Incoherent neutron-scattering structure factors computed for water protons from MD simulations of a hydrated RNase cluster (*dashed line*) and crystal (*solid line*).

(Paciaroni et al., 1998), and subsequently confirmed by difference neutron-scattering measurements on plastocyanin (Paciaroni et al., 1999). After subtraction of the protein contribution, the experimental spectrum of the hydration water at 100 K displayed a boson peak centered at 3 meV, in excellent agreement with our crystal simulation result in Fig. 11. However, in the theoretical plastocyanin spectrum (Paciaroni et al., 1998), computed directly for the water protons in a simulation of a protein/water cluster using the SPC/E water model, the peak occurs at significantly lower energy (1.3 meV). We note a similar discrepancy in our cluster result in Fig. 11, and we interpret it as another indication of the inadequacy of the cluster model for simulating protein hydration water dynamics. The microscopic origins of boson peaks in glassy systems have yet to be definitively described. Simulations could prove useful in the elucidation of boson peak vibrations, and our crystal simulation, which has correctly reproduced the location and the shape of the peak for the first time, provides a useful starting point for further analysis.

Connection between water dynamics and protein structural relaxation

Neutron scattering and other experiments have demonstrated that, below ~200 K, proteins behave dynamically as harmonic solids. The so-called dynamical transition from harmonic to anharmonic and diffusive dynamics as the temperature is raised requires a threshold level of hydration. The magnitude of the additional motions activated at the transition is proportional to the level of hydration (Doster and Settles, 1999), and, in dry proteins, the transition appears to be completely suppressed (Ferrand et al., 1993; Lehnert et al., 1998; Fitter, 1999). The transition temperature is raised by increasing the viscosity of the solvent (Lichtenegger et al., 1999). Very recently, by separately controlling the temperatures of the protein and water in a series of MD simulations, Vitkup et al. (2000) found that solvent mobility was the dominant factor determining protein atomic fluctuations above 180 K. The molecular mechanism of the solvent motion that is required to permit or trigger the protein structural relaxation above the transition temperature has yet to be worked out. In this section, we present a preliminary analysis of our simulations that may provide a direction for further experimental and theoretical investigations of the role of particular water motions in the dynamical transition.

In Fig. 12 *A*, we present incoherent intermediate scattering functions for the protein hydrogen atoms from simulations of the RNase crystal at 150 and 300 K, and the low hydration (dry) powder at 300 K. Consistent with the results of neutron-scattering experiments (Doster et al., 1990), in the 300-K crystal, above the threshold of both hydration and thermal energy required for the dynamical transition, the intermediate scattering function displays a two-stage decay: a fast β relaxation on the time scale of 1 ps, followed by a slower α structural relaxation that sets in roughly on the 50-ps time scale. In contrast, in the dry powder at 300 K, i.e., below the hydration threshold, and in the crystal at 150 K, i.e., below the transition temperature, the β relaxation takes place, but the α relaxation is significantly reduced.

To elucidate the role of water dynamics in activating the protein structural relaxation that accompanies the dynamical transition, we compare the translational and rotational motion of the water molecules in the RNase crystal at 150 and 300 K, and in the dry powder at 300 K. The translational motion is illustrated by the center-of-mass mean-squared displacements plotted in Fig. 12 *A*, and the rotational motion by the water dipole second-rank rotational correlation functions in Fig. 12 *C*. The MSDs in Fig. 12 *B* show that, in the 300-K crystal, diffusive translational motion of the water molecules begins on a time scale of approximately 1

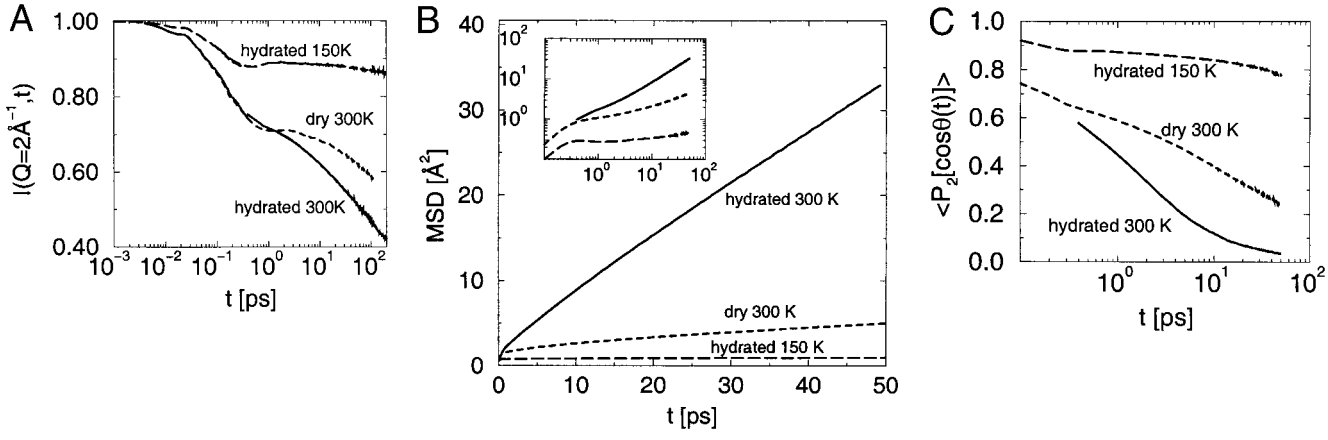

FIGURE 12 Semi-log plots of time correlation functions for RNase hydration water in the crystal at 150 K (*long dashed line*) and 300 K (*solid line*), and the dry powder at 300 K (*short dashed line*): (*A*) intermediate scattering (density correlation) functions for the H atoms; (*B*) center-of-mass mean-squared displacements, also displayed as a log-log plot in the inset; (*C*) second-rank rotational correlation functions for the water dipoles.

ps. In contrast, in the dry powder at 300 K and the crystal at 150 K, the MSDs reach plateaus (or show very slow increases in time), indicating that the water molecules in these systems are confined, trapped by the "cage effect" well known in supercooled liquids (Gallo et al., 1996). In Fig. 12 *C*, the rotational correlation function exhibits nearly complete decay on a time scale of tens of picoseconds in the 300-K crystal, and significant decay in the 300-K dry powder, whereas, in the 150-K crystal, it shows no appreciable decay.

The results in Fig. 12, *A* and *B* may be summarized as follows: on the time scale of tens of picoseconds in the crystal at 300 K, significant water translational diffusion (i.e., beyond the diameter of a water molecule) and rotational motion (reflected in the decay of the rotational correlation function) occur; in the dry powder at 300 K, the water molecules are translationally confined but display appreciable rotational motion; and in the crystal at 150 K, both translational and rotational motion of the water molecules are essentially arrested. These results, along with the fact that the dynamical transition only takes place under conditions of hydration and temperature present in our 300-K crystal, suggest that water translational motion is necessary for the structural relaxation that permits anharmonic and diffusive motions in proteins. Furthermore, it appears that the exchange of protein–water hydrogen bonds by water rotational/librational motion, is not sufficient to permit protein structural relaxation. Rather, it appears that complete exchange of protein-bound water molecules by translational displacement is required. A more complete analysis of the connection of specific water motions to protein dynamics is the subject of an on-going investigation that will be reported elsewhere.

CONCLUSIONS

One of the main goals of this study is to demonstrate that it is possible to obtain a reliable, accurate representation of the picosecond time-scale water dynamics in the vicinity of proteins by means of molecular dynamics simulations, using current-generation atomic force fields. An extensive series of calculations, varying both the protein environment and temperature, has allowed us to clearly demonstrate that simulations of protein hydration performed on "cluster" systems, in which a single protein molecule is surrounded by a finite hydration shell, lead to different water behavior compared with powder environments, where most neutron inelastic experiments are performed. We have also shown that water mobility on the time scale of tens of picoseconds is essentially identical in crystal and powder environments. This original result indicates that dynamical experimental data taken on powder samples are relevant to discussing water dynamics near proteins in native-like environments such as crystals. Regarding the water model considered in the calculation, it appears that results obtained with the SPC/E model are in much better agreement with neutron-scattering experiments than TIP3P. This was clearly demonstrated by the density of states and the dynamical susceptibility, where both the modification of water dynamics from bulk behavior by the protein environment and its temperature dependence were accurately reproduced over a broad frequency range. The overall agreement with neutron data validates the methodologies and potential used, and provides a solid ground for accurately describing the water motion in relation to the protein dynamics and function. We have used our simulation trajectories to examine the common assumption of experimental data reduction that the water rotational and translational motions are decoupled. We found that, in analogy with bulk supercooled water, the coupling in protein hydration water is greatest at higher values of momentum transfer, with the maximum ($\approx$5%) reached at approximately 1 ps at higher temperature (300 K), and much longer times ($>$100 ps) at lower temperature (150 K). Finally, comparing the time scales of protein structural relaxation (as reflected in the secondary decay of $I(Q, t)$) with water translational and rotational motion suggests that protein–water hydrogen bond fluctuations by water rotational motion is insufficient, and translational displacement is required for protein structural relaxation.

D. J. T. acknowledges support of this work by start-up funds from the School of Physical Sciences at the University of California–Irvine, and a grant (ACS-PRF 33247-G7) from the administrators of The Petroleum Research Fund, administered by the American Chemical Society.

REFERENCES

Allen, M. P., and D. J. Tildesley. 1989. Computer Simulation of Liquids. Clarendon Press, Oxford.

Andersen, H. C. 1983. Rattle: a Velocity Version of the Shake Algorithm for Molecular Dynamics Calculations. *J. Comp. Phys.* 52:24–34.

Angell, C. A. 1995. Formation of Glasses from Liquids and Biopolymers. *Science.* 267:1924–1935.

Badger, J., and D. L. D. Caspar. 1991. Water Structure in Cubic Insulin Crystals. *Proc. Natl. Acad. Sci. U. S. A.* 88:622–626.

Barron, L. D., L. Hecht, and G. Wilson. 1997. The Lubricant of Life: A Proposal That Solvent Water Promotes Extremely Fast Conformational Fluctuations in Mobile Heteropolypeptide Structure. *Biochemistry.* 36: 13143–13147.

Beé, M. 1988. Quasielastic Neutron Scattering: Principles and Applications in Solid State Chemistry, Biology, and Materials Science. Adam Hilger, Bristol.

Bellissent-Funel, M. C. 2000. Hydration in Protein Dynamics and Function. *J. Molec. Liq.* 94:39–52.

Bellissent-Funel, M. C., K. F. Bradley, S. H. Chen, J. Lal, and J. Teixeira. 1993. Slow Dynamics of Water Molecules in Confined Space. *Physica A.* 201:277–285.

Bellissent-Funel, M. C., J. M. Zanotti, and S. H. Chen. 1996. Slow Dynamics of Water Molecules on the Surface of a Globular Protein. *Faraday Discuss.* 103:281–294.

Berendsen, H. J. C., J. R. Grigera, and T. P. Straatsma. 1987. The Missing Term in Effective Pair Potentials. *J. Phys. Chem.* 91:6269–6271.

Bizzarri, A. R., and S. Cannistraro. 1996. Molecular Dynamics Simulation Evidence of Anomalous Diffusion of Protein Hydration Water. *Phys. Rev. E.* 53:3040–3043.

Bizzarri, A. R., and S. Cannistraro. 1997. Anomalous and Anisotropic Diffusion of Plastocyanin Hydration Water. *Europhys. Lett.* 37:201–206.

Bizzarri, A. R., C. Rocchi, and S. Cannistraro. 1996. Origin of the Anomalous Diffusion Observed by MD Simulation at the Protein-Water Interface. *Chem. Phys. Lett.* 263:559–566.

Boon, J. P., and S. Yip. 1991. Molecular Hydrodynamics. Dover, New York.

Bryant, R. G. 1996. The Dynamics of Water-Protein Interactions. *Annu. Rev. Biophys. Biomol. Struct.* 25:29–53.

Burling, F. T., W. I. Weis, K. M. Flaherty, and A. T. Brünger. 1996. Direct Observation of Protein Solvation and Discrete Disorder with Experimental Crystallographic Phase. *Science.* 217:72–77.

Chen, S. H., P. Gallo, F. Sciortino, and P. Tartaglia. 1997. Molecular-Dynamics Study of Incoherent Quasielastic Neutron-Scattering Spectra of Supercooled Water. *Phys. Rev. E.* 56:4231–4243.

Cheng, X., and B. P. Schoenborn. 1990. Hydration in Protein Crystals. A Neutron Diffraction Analysis of Carbonmonoxymyoglobin. *Acta Cryst.* B46:195–208.

Denisov, V. P., and B. Halle. 1995:Protein Hydration Dynamics in Aqueous Solution. A Comparison of Bovine Pancreatic Trypsin Inhibitor and Ubiquitin by Oxygen-17. Spin Relaxation Dispersion. *J. Mol. Biol.* 245:682–697.

Denisov, V. P., and B. Halle. 1996. Protein Hydration Dynamics in Aqueous Solution. *Faraday Disc.* 103:227–244.

Denisov, V. P., and B. Halle. 1998. Thermal Denaturation of Ribonuclease A Characterized by Water ^{17}O and ^{2}H Magnetic Relaxation Dispersion. *Biochemistry.* 37:9595–9604.

Doster, W., S. Cusack, and W. Petry. 1990. Dynamical Instability of Liquidlike Motions in a Globular Protein Observed by Inelastic Neutron Scattering. *Phys. Rev. Lett.* 65:1080–1083.

Doster, W., and M. Settles. 1999. The Dynamical Transition in Proteins: The Role of Hydrogen Bonds. *In* Hydration Processes in Biology: Experimental and Theoretical Approaches. M.-C. Bellissent-Funel, editor. IOS Press, Amsterdam. 177–191.

Essmann, U., L. Perera, M. L. Berkowitz, T. Darden, and L. G. Pedersen. 1995. A Smooth Particle Mesh Ewald Method. *J. Chem. Phys.* 103: 8577–8593.

Ferrand, M., A. J. Dianoux, W. Petry, and G. G. Zaccai. 1993. Thermal Motions and Function of Bacteriorhodopsin in Purple Membranes: Effects of Temperature and Hydration Studied by Neutron Scattering. *Proc. Natl. Acad. Sci. U. S. A.* 90:9668–9672.

Fitter, J. 1999. The Temperature Dependence of Internal Molecular Motions in Hydrated and Dry α-Amylase: The Role of Hydration Water in the Dynamical Transition of Proteins. *Biophys. J.* 76:1034–1042.

Fitter, J., R. E. Lechner, and N. A. Dencher. 1997. Picosecond Molecular Motions in Bacteriorhodopsin from Neutron Scattering. *Biophys. J.* 73:2126–2137.

Frick, B., and D. Richter. 1995. The Microscopic Basis of the Glass Transition in Polymers from Neutron Scattering Studies. *Science.* 267: 1939–1945.

Gallo, P., F. Sciortino, P. Tartaglia, and S. H. Chen. 1996. Slow Dynamics of Water Molecules in Supercooled States. *Phys. Rev. Lett.* 76: 2730–2733.

Goldanskii, V. I., and Y. F. Krupyanskii. 1989. Protein and Protein-Bound Water Dynamics Studied by Raleigh Scattering of Mössbauer Radiation (RSMR). *Quart. Rev. Biophys.* 22:39–92.

Halle, B. 1999a. Magnetic Relaxation Dispersion: Principles and Applications. *In* Hydration Processes in Biology: Theoretical and Experimental Approaches. M.-C. Bellissent-Funel, editor. IOS Press, Amsterdam. 221–232.

Halle, B. 1999b. Water in Biological Systems: The NMR Picture. *In* Hydration Processes in Biology: Theoretical and Experimental Approaches. M.-C. Bellissent-Funel, editor. IOS Press, Amsterdam. 233–249.

Jiang, J. S., and A. T. Brünger. 1994. Protein Hydration Observed by X-Ray Diffraction. Solvation Properties of Penicillopepsin and Neuraminidase Crystal Structures. *J. Mol. Biol.* 243:100–115.

Jorgensen, W. L., J. Chandrasekhar, J. D. Madura, R. W. Impey, and M. L. Klein. 1983. Comparison of Simple Potential Functions for Simulating Liquid Water. *J. Chem. Phys.* 79:926–935.

Lehnert, U., V. Réat, M. Weik, G. Zaccaï, and C. Pfister. 1998. Thermal Motion in Bacteriorhodopsin at Different Hydration Levels Studied by Neutron Scattering: Correlation with Kinetics and Light-Induced Conformational Changes. *Biophys. J.* 75:1945–1952.

Leyser, H., W. Doster, and M. Diehl. 1999. Far-Infrared Emission by Boson Peak Vibrations in a Globular Protein. *Phys. Rev. Lett.* 82: 2987–2990.

Lichtenegger, H., W. Doster, T. Kleinert, A. Birk, B. Sepiol, and G. Vogl. 1999. Heme-Solvent Coupling: A Mössbauer Study of Myoglobin in Sucrose. *Biophys. J.* 76:414–422.

MacKerell, Jr., A. D., D. Bashford, M. Bellott, R. L. Dunbrack, Jr., J. Evanseck, M. J. Field, S. Fischer, J. Gao, H. Guo, S. Ha, D. Joseph-McCarthy, L. Kuchnir, K. Kuczera, F. T. K. Lau, C. Mattos, S. Michnick, T. Ngo, D. T. Nguyen, B. Prodhom, W. E. Reiher, I. I. I., B. Roux, M. Schlenkrich, J. C. Smith, R. Stote, J. Straub, M. Watanabe, J. Wiorkiewicz-Kuczera, D. Yin, and M. Karplus. 1998. All-Atom Empirical Potential for Molecular Modeling and Dynamics Studies of Proteins. *J. Phys. Chem. B.* 102:3586–3616.

Martyna, G. J., D. J. Tobias, and M. L. Klein. 1994. Constant Pressure Molecular Dynamics Simulations. *J. Chem. Phys.* 101:4177–4189.

Martyna, G. J., M. E. Tuckerman, and M. L. Klein. 1992. Nosé-Hoover Chains: the Canonical Ensemble via Continuous Dynamics. *J. Chem. Phys.* 97:2635–2643.

Martyna, G. J., M. E. Tuckerman, D. J. Tobias, and M. L. Klein. 1996. Explicit Reversible Integrators for Extended Systems Dynamics. *Molec. Phys.* 87:1117–1157.

Meyer, E. 1992. Internal Water Molecules and H-Bonding in Biological Macromolecules: A Review of Structural Features with Functional Implications. *Protein Sci.* 1:1543–1562.

Middendorf, H. D. 1984. Biophysical Applications of Quasi-elastic and Inelastic Neutron Scattering. *Ann. Rev. Biophys. Bioeng.* 13:425–451.

Middendorf, H. D. 1996. Neutron Studies of the Dynamics of Biological Water. *Physica B.* 226:113–127.

Otting, G. 1997. NMR Studies of Water Bound to Biological Molecules. *Prog. NMR Spect.* 31:259–285.

Otting, G., E. Liepinsh, and K. Wüthrich. 1991. Protein Hydration in Aqueous Solution. *Science.* 254:974–980.

Otting, G., and K. Wüthrich. 1989. Studies of Protein Hydration in Aqueous Solution by Direct NMR Observation of Individual Protein-Bound Water Molecules. *J. Am. Chem. Soc.* 111:1871–1875.

Paciaroni, A., A. R. Bizzarri, and S. Cannistraro. 1998. Molecular-Dynamics Simulation Evidences of a Boson Peak in Protein Hydration Water. *Phys. Rev. E.* 57:6277–6280.

Paciaroni, A., A. R. Bizzarri, and S. Cannistraro. 1999. Neutron Scattering Evidence of a Boson Peak in Protein Hydration Water. *Phys. Rev. E.* 60:2476–2479.

Phillips, G. N., and B. M. Pettitt. 1995. Structure and Dynamics of the Water Around Myoglobin. *Protein Sci.* 4:149–158.

Polnaszek, C. F., and R. G. Bryant. 1984. Nitroxide Radical Induced Solvent Proton Relaxation: Measurements of Localized Translational Diffusion. *J. Chem. Phys.* 81:4038–4045.

Randall, J., H. D. Middendorf, H. L. Crespi, and A. D. Taylor. 1978. Dynamics of Protein Hydration by Quasi-elastic Neutron Scattering. *Nature.* 276:636–638.

Rasmussen, B. F., A. M. Stock, D. Ringe, and G. A. Petsko. 1992. Crystalline Ribonuclease A Loses Function Below the Dynamical Transition at 220 K. *Nature.* 357:423–424.

Rocchi, C., A. R. Bizzarri, and S. Cannistraro. 1998. Water Dynamical Anomalies Evidenced by Molecular-Dynamics Simulations at the Solvent-Protein Interface. *Phys. Rev. E.* 57:3315–3325.

Rupley, J. A., and G. Careri. 1991. Protein Hydration and Function. *Adv. Protein Chem.* 41:37–172.

Ryckaert, J.-P., G. Ciccotti, and H. J. C. Berendsen. 1977. Numerical Integration of the Cartesian Equations of Motion of a System with

Constraints: Molecular Dynamics of *n*-Alkanes. *J. Comp. Phys.* 23: 327–341.

Settles, M., and W. Doster. 1996. Anomalous Diffusion of Adsorbed Water: A Neutron Scattering Study of Hydrated Myoglobin. *Faraday Discuss.* 103:269–279.

Steinhoff, H. J., B. Kramm, G. Hess, C. Owerdieck, and A. Redhardt. 1993. Rotational and Translational Water Diffusion in the Hemoglobin Hydration Shell. *Biophys. J.* 65:1486–1495.

Tarek, M., and D. J. Tobias. 1999. Environmental Dependence of the Dynamics of Protein Hydration Water. *J. Am. Chem. Soc.* 121: 9740–9741.

Teeter, M. M. 1991. Water-Protein Interactions: Theory and Experiment. *Ann. Rev. Biophys. Chem.* 20:577–600.

Tilton, Jr., R. F., J. C. Dewan, and G. A. Petsko. 1992. Effect of Temperature on Protein Structure and Dynamics: X-ray Crystallographic Studies of the Protein Ribonuclease-A at Nine Different Temperatures from 98 to 320 K. *Biochemistry.* 31:2469–2481.

Vitkup, D., D. Ringe, G. A. Petsko, and M. Karplus. 2000. Solvent Mobility and the Protein 'Glass' Transition. *Nature Struct. Biol.* 7:34–38.

Weast, R. C. 1971. Handbook of Chemistry and Physics. CRC Press, Boca Raton.

Williams, M. A., J. M. Goodfellow, and J. M. Thornton. 1994. Buried Waters and Internal Cavities in Monomeric Proteins. *Protein Sci.* 3:1224–1235.

Wlodawer, A. 1982. Neutron Protein Crystallography. *Prog. Biophys. Mol. Biol.* 40:115–157.

Wlodawer, A., L. A. Svensson, L. Sjolin, and G. Gilliland. 1988. Structure of Phosphate Free Ribonuclease A Refined at 1.26 Å Resolution. *Biochemistry.* 27:2705–2717.

Zanotti, J. M., M. C. Bellissent-Funel, and S. H. Chen. 1999. Relaxational Dynamics of Supercooled Water in Porous Glass. *Phys. Rev. E.* 59: 3084–3093.